Semiconductor–metal transition of pyrite FeS_2 under high pressure by full-potential linearized-augmented plane wave calculations

2006 J. Phys.: Condens. Matter 18 9151

(http://iopscience.iop.org/0953-8984/18/40/002)

INSTITUTE OF PHYSICS PUBLISHING JOURNAL OF PHYSICS: CONDENSED MATTER

J. Phys.: Condens. Matter **18** (2006) 9151–9160 doi:10.1088/0953-8984/18/40/002

Semiconductor–metal transition of pyrite FeS_2 under high pressure by full-potential linearized-augmented plane wave calculations

J Cai[1], **I Goliney**[2] **and M R Philpott**[2]

[1] Department of Physics, Tsinghua University, Beijing 100084, People's Republic of China
[2] Department of Materials Science, National University of Singapore, 119260, Singapore

Received 1 June 2006, in final form 29 August 2006
Published 22 September 2006
Online at stacks.iop.org/JPhysCM/18/9151

Abstract

The effects of hydrostatic pressure on the electronic band structure of the semiconductor mineral iron pyrite FeS_2 have been investigated theoretically by an *ab initio* full-potential linearized-augmented plane wave (FPLAPW) method within a local approximation (LDA/GGA) to the density functional theory. The calculations predict that at a pressure of 94.1 GPa the indirect band gap of pyrite FeS_2 vanishes and the material becomes a metal. This is due to the presence of the S–S and Fe–S bonds, which provide novel energy band distortions in the process of attaining the metallic state. Analysis indicates that, under increasing high pressure, the conduction bands ($3p_z$ of sulfur and $3d_{x^2-y^2} + 3d_{xy}$ of iron) intrude downwards into the valence bands, which are predominantly 3d in nature. At normal pressure, the lattice constant, the bulk modulus, sulfur position parameter u, S–S bond length, and the indirect band gap of pyrite FeS_2 are calculated using a fully relaxed unit cell and found to be equal to 541.8 pm, 159.7 GPa, $u = 0.383$, 219.5 pm and 0.45 eV, respectively. Apart from the gap, which is too small (the usual 'LDA error'), these results agree well with recent experiments. The effective masses of an electron at selected points in the conduction band are reported.

(Some figures in this article are in colour only in the electronic version)

1. Introduction

Iron pyrite belongs to the transition-metal dichalcogenides, which display a broad range of optical, magnetic, and electronic properties [1–6] that, in the past, made them potentially attractive for various technological applications, including solid-state batteries and photovoltaic materials for solar cells. They are also the materials of potential choice for devices in which long minority carrier recombination lifetimes are beneficial. Current interest in materials of this class is connected with the search for S poisoning resistant catalysts [7], re-mediating the

environmental impact of acid mine drainage as a result of oxidation of pyrite minerals [8, 9], and scenarios concerning the mineral origins of life on Earth [10–12].

Iron pyrite, FeS_2, is known to be a non-magnetic semiconductor and its electronic structure has been extensively investigated both theoretically and experimentally at room temperature and pressure [1–6, 13–17]. There have been several reports of experiments performed at high pressure [13–18]. Yet the electronic structure of pyrite FeS_2 under pressure has not been investigated theoretically with full relaxation of both the lattice constant and the sulfur position parameter.

Almost 30 years ago Schlegel and Wachter [13] reported a personal communication from Batlogg that the band gap of iron pyrite shifted to the blue when an external pressure was applied to crystalline samples. On the basis of a theoretical calculation, Eyert *et al* [14] proposed that the blue shift is generated by a change in sulfur position in the FeS_2 lattice. Central to their explanation was the proposal that the positional parameter of sulfur should increase with pressure. However, this explanation is not in accord with the experimental compression data [15, 16]. Recent total energy calculations using density function theory by Opahle *et al* [15] predicted a red shift of the fundamental absorption edge with increasing pressure. This theoretical prediction is in agreement with the recent experimental observation of Cervantes *et al* [17], who found that the band gap had a red-shift under pressure [17]. Furthermore, Opahle *et al* [15] attributed the experimental blue shift reported by Batlogg [13] to a pseudo-gap behaviour. They argued that the observed absorption edge was due to the transitions between the occupied non-bonding Fe 3d states and unoccupied hybridized Fe 3d–S 3p states, which shift slightly toward higher energies under pressure, while the red-shift of the band gap is determined by the unoccupied optically inactive S $3p_z$ band, the energy of which decreases with increasing pressure. These authors also noted that, by allowing the lattice parameters to relax during the minimizing of the total energy of the crystal, the band gap of pyrite FeS_2 vanished [15] at zero pressure. This is completely contrary to the widely held view based on numerous experiments that iron pyrite is an indirect semiconductor with a band gap in the range 0.9–0.95 eV [15, 16, 19–21].

The present work clarifies the issues of the band gap width, the effective mass of the electron in the conduction band and a possible semiconductor–metal transition by studying the electronic structure of iron pyrite as a function of pressure using a full-potential linearized-augmented plane wave (FPLAPW) method [22]. The calculations reported here confirm the theoretical decrease in the pyrite's band gap under pressure. We also show that FeS_2 is transformed from a semiconductor into a metal under high pressure by a novel electron band distortion mechanism.

In section 2, the theoretical method is introduced. Then, in section 3, the results and discussions are given including an interpretation of changes in calculated electron density for low and high pressures. Finally, we summarize our conclusions in section 4.

2. Theory and method

Self-consistent band structure calculations for FeS_2 crystals are performed using the WIEN2k code [22]. This code is based on the application of the FPLAPW method [22]. Like most energy band methods, the linearized-augmented plane wave method is a procedure for solving the Kohn–Sham equations for the ground-state density, total energy, and eigenvalues of a many-electron system by introducing a basis set which is especially adapted to the particular problem. This adaptation is achieved by dividing the unit cell into non-overlapping atomic spheres and an interstitial region. In the two types of regions, different basis sets are used. Inside the atomic spheres with muffin tin radii R_{MT}, a linear combination of the radial function times

spherical harmonics is used. The radial function is the regular solution of the radial Schrödinger equation. In the interstitial region, a plane wave expansion is used. The crystal potential, the electronic wavefunctions, and the charge densities are also expanded differently in these two regions. Thus, no shape approximations are made. Such a procedure is frequently called a 'full-potential' method. The method is described in detail, for example, in the paper by Blaha *et al* [23].

Using the FPLAPW method, we solved the Kohn–Sham equations for the electronic structure of iron pyrite as a function of pressure (1000 k points for the first Brillouin zone). The exchange and correlation potential are taken in the form of a generalized gradient approximation of Perdew *et al* [24]. We have chosen muffin tin radii $R_{MT} = 190.0$ pm for Fe and 175.0 pm for S atoms. Inside the atomic spheres, waves are expanded up to the maximum angular quantum number $l_{max} = 10$, while the number of plane waves in the interstitial region is limited by the cutoff at $k_{max} = 7.0/R_{min}$, where R_{min} is the smallest of all atomic muffin tin radii. The charge density is Fourier expanded up to the maximum wavevector $G_{max} = 14$. In the process of solving the Dirac equation, the atomic valence states are treated within the scalar-relativistic approach while the core states are relaxed in a fully relativistic manner. The SRA means a technique for the reduction of the Dirac equation which initially omits the spin–orbit interaction but retains all other relativistic kinematic effects such as mass–velocity, Darwin and higher-order terms [25].

3. Results and discussions

Crystalline iron pyrite, FeS_2, has a formal similarity to the NaCl rock-salt structure. In pyrite structure, the Fe atoms form an fcc sublattice similar to the sodium lattice in NaCl. Instead of a single chloride ion on the sites of the complementary fcc lattice in rock-salt, there are S–S pairs oriented in one of four possible $\langle 111 \rangle$ direction. Consequently, the pyrite unit cell contains four formula units ($Z = 4$). Each iron is surrounded by six sulfur atoms, and each sulfur is bonded to another sulfur atom and three iron atoms.

There are 24 symmetry operations in the $Pa\bar{3}(T_h^6)$ space group of FeS_2. The four iron atoms are located at positions $(0, 0, 0)$, $(0, 1/2, 1/2)$, $(1/2, 0, 1/2)$, and $(1/2, 1/2, 0)$. The eight sulfur atoms are at positions $\pm(u, u, u)$, $\pm(1/2-u, -u, 1/2+u)$, $\pm(-u, 1/2+u, 1/2-u)$, and $\pm(1/2+u, 1/2-u, -u)$, where u is the position parameter of sulfur. The two lattice parameters (lattice constant a and sulfur's position parameter u) are related to the distance d_{S-S} between two sulfur atoms in a pair by the formula $d_{S-S} = \sqrt{3}(1-2u)a$.

Most of the published calculations for the electronic structure of iron pyrite were performed using the experimental lattice parameters. In order to compare our numerical results with previous calculations, we also first calculated the electronic structure of FeS_2 with an experimental lattice period of 541.6 pm and sulfur position parameter $u = 0.386$ [26]. In this calculation we obtained a band gap of 0.85 eV, which agrees quite well with other computational results: 0.85 eV by Opahle *et al* [15] and 0.90 eV by Eyert *et al* [14].

We then calculated the electronic structure of FeS_2 by optimizing the sulfur position parameter u and the lattice period. In figures 1 and 2, respectively, we show the variation in total energy and position parameter u with the unit cell volume. We obtained an equilibrium lattice period and positional parameter of sulfur of 541.8 pm and 0.383, respectively. Thus, upon relaxation the lattice, expanded slightly (a changed from 541.6 to 541.8 pm) and the sulfur atoms in each pair moved proportionally more apart (u relaxed from 0.386 to 0.383). The values reported by Ohpale *et al* in [15] differ quite significantly. If our positional parameter was by 0.8% off the experemental value, the same parameter in [15] was 2% smaller. Both Ohpale and Zeng obtained quite high values for the S–S distance (225 pm in [15] and 230 pm

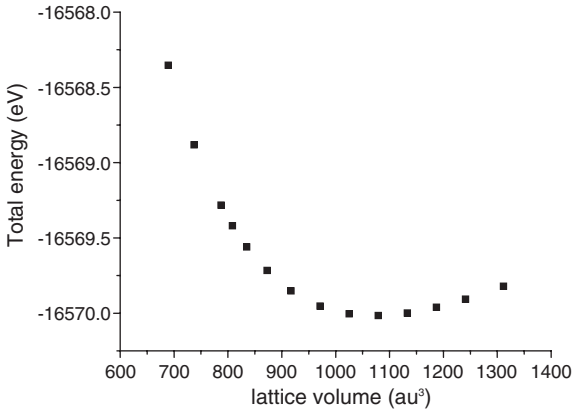

Figure 1. Total energy versus lattice constant for a pyrite crystal. The theoretical equilibrium lattice constant is 541.8 pm.

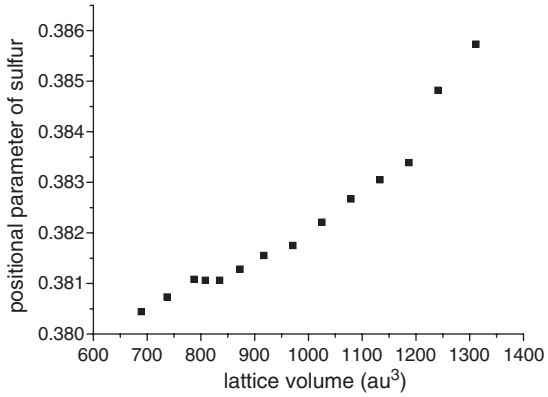

Figure 2. Position parameter of sulfur versus lattice constant for FeS_2. The theoretical equilibrium state of the semiconductor pyrite corresponds to a lattice constant of 541.8 pm, and the transition state of pyrite from semiconductor to metal corresponds to a lattice constant of 408.0 pm.

in [27] compared to the experimental value of 216 pm). Yet, an accurate prediction of the distance between the sulfur atoms in an S–S pair is critical both for the band structure and the determination of the band gap. Evidence for this is the fact that all workers obtained more realistic values of the band gap for the experimental lattice parameters. The S–S distance of 219.5 pm obtained in our calculations is still larger than the experimental value.

From the second derivative of the total energy curve in figure 1 we obtained a bulk modulus B of FeS_2. The calculated value $B = 159.7$ GPa is about 10% higher than the literature value $B = 145$ GPa deduced from ultrasound measurements [19]. The value of $B = 185$ GPa reported by Opahle *et al* [15] is about 30% higher than the experimental value. As various experiments with different methods reported bulk moduli B ranging from 118 to 162 GPa [16, 20], we may state that our result is in the higher end of the experimental range.

We also calculated the band gap and the electron effective mass in the conduction band for the equilibrium state, where FeS_2 is at zero pressure and has optimized lattice parameters ($a = 541.8$ pm, $u = 0.383$). In figure 3 we show the calculated band structure of the pyrite FeS_2 along selected high-symmetry lines and in figure 4 the calculated total density of states

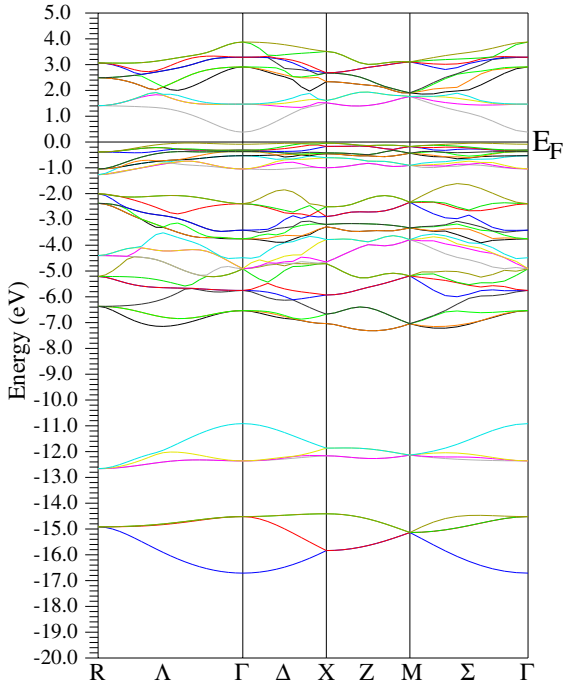

Figure 3. Band structure of pyrite at zero pressure, where different states are recognized by the different colour lines. E_F denotes the Fermi level. The lowest conduction-band edge is mainly composed of S $3p_z$ orbitals.

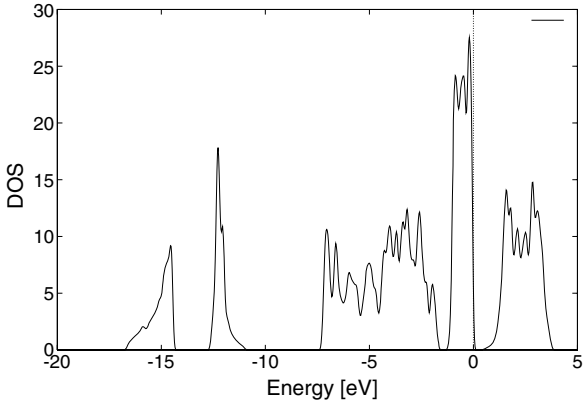

Figure 4. Total density of states of pyrite at zero pressure. The dashed line shows the Fermi level and the lowest conduction-band edge is mainly composed of S $3p_z$ orbitals.

(DOS). In the band structure, see figure 3, the valence band maximum is located close to the X point and the conduction-band minimum is at the Γ point. The indirect band gap between these two points is calculated to be $E_g = 0.45$ eV, compared to 0.85 eV for the unrelaxed structure. The change in the crystal lattice parameters a and u might seem very small, yet the band gap width turns out to be very sensitive to these values, especially to the value of the S–S bond length.

The experimental values of the FeS_2 band gap varies in a broad range from 0.7 to 2.62 eV [15, 16, 19, 20]. The most reliable values obtained from the photo-conductivity measurements appear to be approximately 0.9 to 0.95 eV [15, 16, 19–21]. The present calculated result is about half the experimental value. The density functional method, being a theory of the ground state, usually does not give accurate values for the band gap of semiconductors. Opahle *et al* [15] also performed calculations for the FeS_2 band structure using their own optimized lattice parameters ($a = 530.2$ pm, $u = 0.377$) and reported that the bulk band gap of FeS_2 was vanishingly small. Using theoretical lattice parameters minimizing the total energy, Zeng *et al* [27] reported a similar result. Our numerical result agrees better with the experiments, but the value of the predicted band gap is only half of what is observed in the photo-conductivity.

Due to the degeneracy of the top valence band states (see figure 3), the structure of the valence bands is far more complex than the conduction band. It is evident though that the valance band (like all bands that arise from the crystal field split Fe 3d states) is narrow (a bandwidth of the order of 0.5 eV) while the predominantly S $3p_z$ conduction band is wider (1 eV) with an isotropic effective mass of 0.37 m_0 at the Γ-point. Note that these local orbitals, like the $3p_x$ $3p_y$ $3p_z$ of Fe and S, are defined by a local coordinate system from local rotation matrices [22]. For example, for Fe, x, y, z are along the cubic axes; for S, the Z-axis is along the S–S direction.

Figure 4 shows the total density of states of iron pyrite at the equilibrium state (zero pressure). We can see that the band structure is split into five groups of bands in the range between -17 and 4 eV. The character of the bands can be evaluated using the partial density of states, which will not be shown in the paper. The two groups between -10 and -17 eV are mostly S 3s states, which form bonding and anti-bonding subsets. A similar density of states was also found in the calculations of previous workers [15] and is consistent with the x-ray photo-electron spectroscopy of core levels reported by van der Heide *et al* [28]. The next group of bands in the range between -7.5 and -1.5 eV below the Fermi level is formed by hybridized S 3p and Fe 3d states, with the main contribution from the S 3p. The upper valence bands are formed by Fe 3d and S 3p states, and the main contribution is from the Fe 3d states. The conduction band is formed mainly by hybridized Fe 3d and S 3p, while the lowest edge of the conduction band is almost exclusively due to S $3p_z$ orbitals without any contributions from the other two S 3p or the Fe 3d orbitals. A close interaction of the S–S pairs is responsible for the the bonding–antibonding coupling of S $3p_z$ states (see [14]). These results are in good agreement with the calculations of Opahle *et al* [15].

We found that the band gap of FeS_2 is very sensitive to the variation of the position parameter of sulfur u. At the equilibrium lattice period, reducing the sulfur position parameter by 0.003 leads to a reduction of 0.40 eV in the band gap. Similar observations were reported by Opahle *et al* [15] and Eyert *et al* [14]. Opahle *et al* [15] found that a reduction of 0.009 in the positional parameter of sulfur in FeS_2 with an optimized lattice constant leads to a decrease in the band gap by at least 0.85 eV. Eyert *et al* [14] reported a large red-shift of the band gap of about 0.67 eV when going from $u = 0.388\,84$ to $0.380\,84$ at the fixed lattice constant of 541.6 pm.

As seen in figure 2, the positional parameter of sulfur gradually reduces on decreasing the lattice period. However, as seen in the figure, in a small interval from the lattice lattice constant of $a = 482.0$ pm to the lattice constant of $a = 491.5$ pm, the positional parameter of sulfur remains almost constant at $u = 0.381$ and forms a plateau. This small range (the plateau) corresponds to the region of phase transition of iron pyrite from the semiconductor to the metal state. In this region, when the external pressure reaches 94.1 GPa (corresponding to a lattice period of 482.0 pm and a sulfur positional parameter of 0.381) the band gap of FeS_2

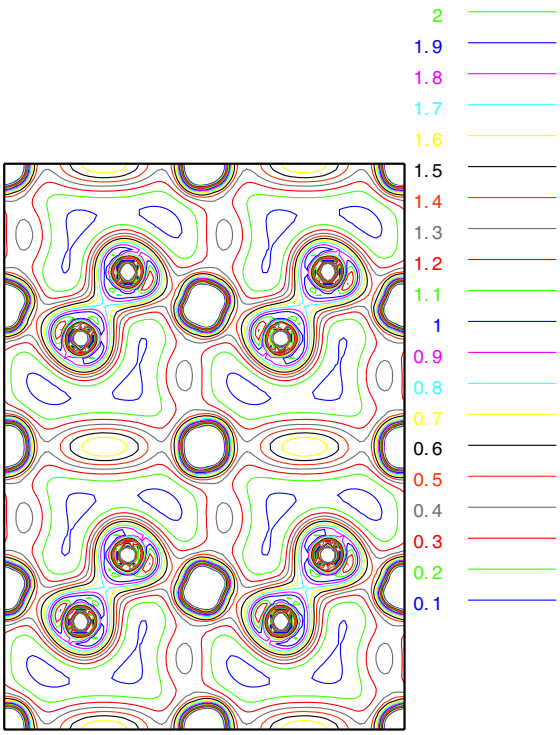

Figure 5. Contour plot of electron density in (110) plane for FeS_2 at zero pressure. The large circles show the Fe atoms, and the small circles indicate S atoms.

decreases from 0.45 eV to zero. This suggests that the semiconductor transforms into a metal (for convenience, henceforth we refer to the two phases as the semiconductor pyrite and the metal pyrite). We believe that the plateau in the dependence of u on cell volume happens due to a stronger mixing and repulsion between the valence bands (mainly Fe 3d and S 3p) and the conduction band (mainly S $3p_z$). The mixing creates an additional force to stabilize the S–S pair and the Fe–S pair relative to the lattice period and results in a plateau in the positional parameter u dependence on the unit cell volume.

The semiconductor–metal transformation is also supported by figures 5 and 6. As seen from these two figures, there is a far greater electron density in the interstitial region for metal pyrite than in the corresponding region for semiconducting FeS_2. For example, for the equilibrium state (zero pressure) in the interstitial region along the $\langle 001 \rangle$ direction between Fe atoms (see figure 5) the value of the electron density is 0.4×10^{-6} pm^{-3}. Along the $\langle 110 \rangle$ between Fe atoms (see figure 5) the value of the electron density is 0.7×10^{-6} pm^{-3}. There is an 'L' shaped interstitial electron region in the top left corner of figure 5. In this region for the semiconductor pyrite the value of electron density is 0.1×10^{-6} pm^{-3}. For the metal pyrite (see figure 6) in the corresponding regions the electron density values are 0.7×10^{-6}, 1.2×10^{-6} and 0.2×10^{-6} pm^{-3}, respectively. The charge density in interstitial regions of metal pyrite is larger than in similar regions of semiconducting pyrite.

The pressure effect on the width of the indirect band gap of iron pyrite was measured experimentally by Cervantes *et al* [17] up to 34 GPa. They found that the band gap of FeS_2 decreases linearly with pressure. They concluded that, if this trend continued linearly, pyrite was expected to metallize at a pressure of 80($\pm$8) GPa. This extrapolated value of pressure

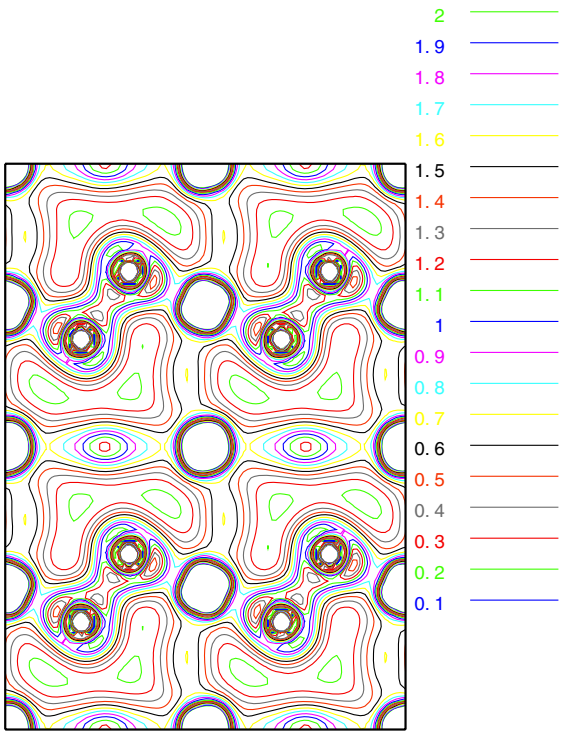

Figure 6. Contour plot of electron density in (110) plane for FeS_2 at a pressure of 94.1 GPa, at which a transition to the metal phase occurs. The electron density in the interstitial region for metal pyrite is much higher than the electron density for semiconducting pyrite at similar points (compare with figure 5).

is in good agreement with the present theoretical prediction of metallization at a pressure of 94.1 GPa.

Finally, we analysed the contributions of different energy bands to the vanishing of the band gap under pressure. Figures 7 and 8 show the band structure and total density of states for FeS_2 under a high pressure of 94.1 GPa (metal pyrite). We find that the conduction bands of the metal FeS_2 have been expanded downwards in energy into the valence bands, as can be seen clearly in figure 7. Figures 7 and 8 clearly show that, under pressure, all of energy bands have been expanded so that the sub-bands of Fe 3d and the sub-bands of S 3p strongly mix not only in the region of energies near the band gap but also in the deeper bands.

By analysing the partial density of states (not shown here) we found that, in the metal pyrite, the lowest edge of the conduction band comes from not only the S $3P_z$ orbital but also Fe $3d_{x^2-y^2} + 3d_{xy}$ orbitals, while the valence-band edge is composed of Fe 3d with a small mixture of S 3p. This feature of the lowest edge of the conduction band is very different from semiconducting pyrite, where the band gap is relatively large and the mixing of Fe 3d and S 3p bands is weak. For the equilibrium state, the lowest edge of the conduction band is determined by S $3p_z$ orbitals.

We found that, with increasing pressure, the contribution of Fe $3d_{x^2-y^2} + 3d_{xy}$ states to the lowest edge of the conduction band gradually increases. This mixing increases the rate of electron transfer and correspondingly decreases the value of the effective electron mass to

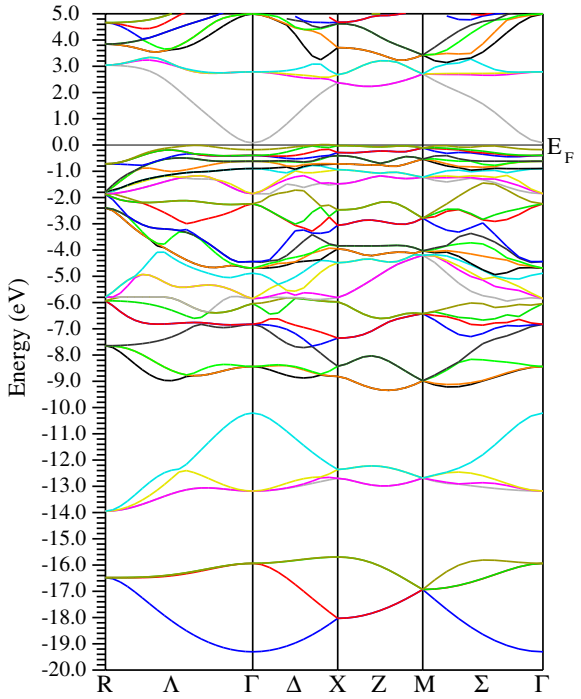

Figure 7. Band structure of pyrite in the metal state, where different states are recognized by the different colours lines. E_F denotes the Fermi level. The lowest conduction-band edge is a mixing of the Fe $3d_{x^2-y^2} + 3d_{xy}$ state and S $3p_z$ state. The bottom of the conduction-band edge overlaps with the top of the valence band.

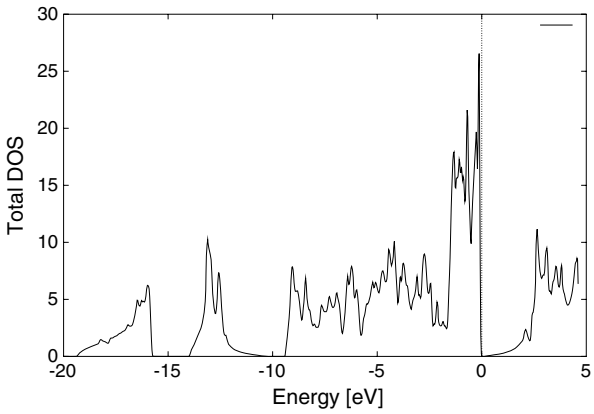

Figure 8. Total density of states of the pyrite in the metallic phase. The dashed line indicates the Fermi level. The lowest conduction-band edge is a mixture of the Fe $3d_{x^2-y^2} + 3d_{xy}$ state and the S $3p_z$ state. The bottom of the conduction-band edge overlaps with the top of the valence band.

0.2 m_0. An increased mixing of Fe $3d_{x^2-y^2} + 3d_{xy}$ states with S $3p_z$ states indicates that a decrease in the Fe–S distance with increasing pressure contributes to the band gap width more and more strongly as the crystal approaches the metallic phase.

4. Conclusions

Using the full-potential linearized-augmented plane wave method, we have studied the electronic structure of iron pyrite under pressure. First, we calculated the lattice period, the bulk modulus, the positional parameter of sulfur, S–S bond length, and the indirect energy gap by optimizing lattice parameters. The corresponding values are 541.8 pm, 159.7 GPa, 0.383, 219.5 pm and 0.45 eV, respectively. These results are in reasonable agreement with experimental values. Most importantly, our calculations show that the unstressed iron pyrite has a finite band gap and it vanishes at the high pressure of 94 GPa. Because at the pressure of 94 Gpa the indirect band gap of pyrite vanishes and the semiconductor pyrite transforms into a metal pyrite. This transformation happens due to the expansion of the conduction bands ($3p_z$ orbital of sulfur and $3d_{x^2-y^2} + 3d_{xy}$ of iron) into the valence bands (3d of iron and 3p of sulfur). With increasing pressure the role of Fe–S distance in the formation of the band gap becomes more important as the Fe and S orbitals mix stronger. Under pressure the electron effective mass significantly decreases. We may conclude also that the theoretical band structure of pyrite is extremely sensitive to the ability of the computational method to predict correct distance between the sulfurs in an S–S pair.

References

[1] Munson R A, DeSorbo W and Kouvel J S 1967 *J. Chem. Phys.* **47** 1769
[2] Bither T A, Bouchard R J, Cloud W H, Donohue P C and Siemons W J 1968 *Inorg. Chem.* **7** 2208
[3] Jarrett H S, Cloud W H, Bouchard R J, Butler S R, Frederick C G and Gillson J L 1968 *Phys. Rev. Lett.* **21** 617
[4] Wilson J A and Yoffe A D 1969 *Adv. Phys.* **18** 193
[5] Ogawa S, Waki S and Teranishi T 1974 *Int. J. Magn.* **5** 349
[6] Kikuchi K, Miyadai T, Itoh H and Fukui T 1978 *J. Phys. Soc. Japan* **45** 444
[7] Somorjai G A 1994 *Introduction to Surface Chemistry and Catalysis* (New York: Wiley) chapter 7, p 451
[8] Langmuir D 1997 *Aqueous Environmental Geochemistry* (Englewood Cliffs, NJ: Prentice-Hall) chapter 11, p 403
[9] Stumm W and Morgan J J 1996 *Aquatic Chemistry* (New York: Wiley–Interscience) chapter 11, p 690
[10] Wächtershäuser G 1988 *Microbiol. Rev.* **52** 452
[11] Cairns-Smith A G, Hall A J and Russell M J 1992 *Orig. Life Evol. Biosph.* **22** 161
[12] Waren A, Bengtson S, Goffredi S K and van Dover C 2003 *Science* **302** 1007
[13] Schlegel A and Wachter P 1976 *J. Phys. C: Solid State Phys.* **9** 3363
[14] Eyert V, Hock K-H, Fiechter S and Tributsch H 1998 *Phys. Rev.* B **57** 6350
[15] Opahle I, Koepernik K and Eschrig H 1999 *Phys. Rev.* B **60** 14035
[16] Will G, Lauterjung J, Schmitz H and Hinze E 1984 *High Pressure in Science and Technology* (*Materials Research Society Symp. Proc.* vol 22) ed C Homan, R K MacCrone and E Whalley (New York: Elsevier) p 49
[17] Cervantes P, Slanic Z, Bridges F, Knittle E and Williams Q 2002 *J. Phys. Chem. Solids* **63** 1927
[18] Mori N and Takahashi H 1987 *High-pressure Research in Mineral Physics* ed Y Syono and M H Manghnani (Tokyo: Terra Scientific Publishing Company) p 341
[19] Blachnik R, Kovitnik S, Steinmeier O, Wilke A, Feltz A, Renter H and Stieber E 1998 *D'Ans-Lax, Taschenbuch fur Chemiker und Physiker* vol III (Berlin: Springer)
[20] Ahrens T J and Jeanloz R 1987 *J. Geophys. Res.* **29** 10363
[21] Ferrer I J, Nevskaia D M, de las Heras C and Sanchez C 1990 *Solid State Commun.* **74** 913
[22] Blaha P, Schwarz K, Madsen G K H, Kvasnicka D and Luitz J 2001 *WIEN2k, An Augmented Plane Wave + Local Orbitals Program for Calculating Crystal Properties* Karlheinz Schwarz, Techn. Univ. Wein, Austria (ISBN 3-9501031-1-2)
[23] Blaha P, Schwarz K, Sorantin P and Trickey S B 1990 *Comput. Phys. Commun.* **59** 399
[24] Perdew J P, Burke S and Ernzerhof M 1996 *Phys. Rev. Lett.* **77** 3865
[25] Koeling D D and Harmon B N 1977 *J. Phys. C: Solid State Phys.* **10** 3107
[26] Stevens E D, DeLucia M L and Coppens P 1980 *Inorg. Chem.* **19** 813
[27] Zeng Y and Holzwarth N A W 1994 *Phys. Rev.* B **50** 8214
[28] van der Heide H, Hemmel R, van Bruggen C F and Haas C 1980 *J. Solid State Chem.* **33** 17